Material Characterization Using Time Domain System

EE4730 High Frequency Wireless Architectures

Petar V. Peshev, p.v.peshev@student.tudelft.nl
Department of Electrical Engineering, Mathematics, and Computer Science,
Delft University of Technology, Delft, The Netherlands

Abstract

Non-destructive spectroscopy is a process in which the permittivity and loss tangent of a material are evaluated without destroying or damaging the sample. It is performed using a time domain system consisting of a fast laser, moving mirror, transmission and receiver photo-conductive antennas, analog-to-digital converter, and measurement computer. Using this setup, the delay and attenuation caused by a sample, at terahertz frequencies, can be compared to a reference signal when no sample is present. By using the delay, the material's permittivity is evaluated, while by using the attenuation and a transmission line model for dielectric in free space, the loss tangent is evaluated.

I. Terahertz Beam-Path Alignment

The setup consists of the transmission and reception photo-conductive antennas (PCAs) and four lenses. The first and third mirrors collimate laser, while the second and fourth focus it. Consequently, the rays should be collimated between the first-second and third-fourth mirror, while focused at the center pinhole (where the sample is positioned). Any miss-alignment in the setup results in smaller received power, therefore, an important step is to align the lenses, in order to increase the received power. The maximum amplitude the received signal can have is around 6 V, good alignment is considered at amplitude of 5 V.

At the start of the alignment, good positions for the PCAs and lenses are provided in Table.I. Moreover, the beams are linearly polarized, therefore, in case the PCAs and lenses are not parallel, the performance is affected.

TABLE I
Initial positions for the time domain system setup.

PCAs and Lenses Initial Positions	
	Distance
Emitter	35 mm
TPX50 1	70 mm
TPX50 2	190 mm
Pinhole	245 mm
TPX50 3	305 mm
TPX50 4	400 mm
Detector	435 mm

After alignment, the final distances for the lenses are summarized in Table.II. In this setup, the diameter of the iris (pinhole) at which the signal starts to attenuate is around 9 mm, therefore, the sample must have a diameter of at least 9 mm, in order for correct material characterization. For these positions, the reference signal is plotted in Fig.1. The achieved pulse response is around 5.3 V. Finally, an overall image of the PCAs and lens setup is shown in Fig.2.

TABLE II
Final positions for the time domain system setup.

PCAs and Lenses Final Positions	
	Distance
Emitter	34.5 mm
TPX50 1	71 mm
TPX50 2	186 mm
Pinhole	245 mm
TPX50 3	292 mm
TPX50 4	415 mm
Detector	462 mm

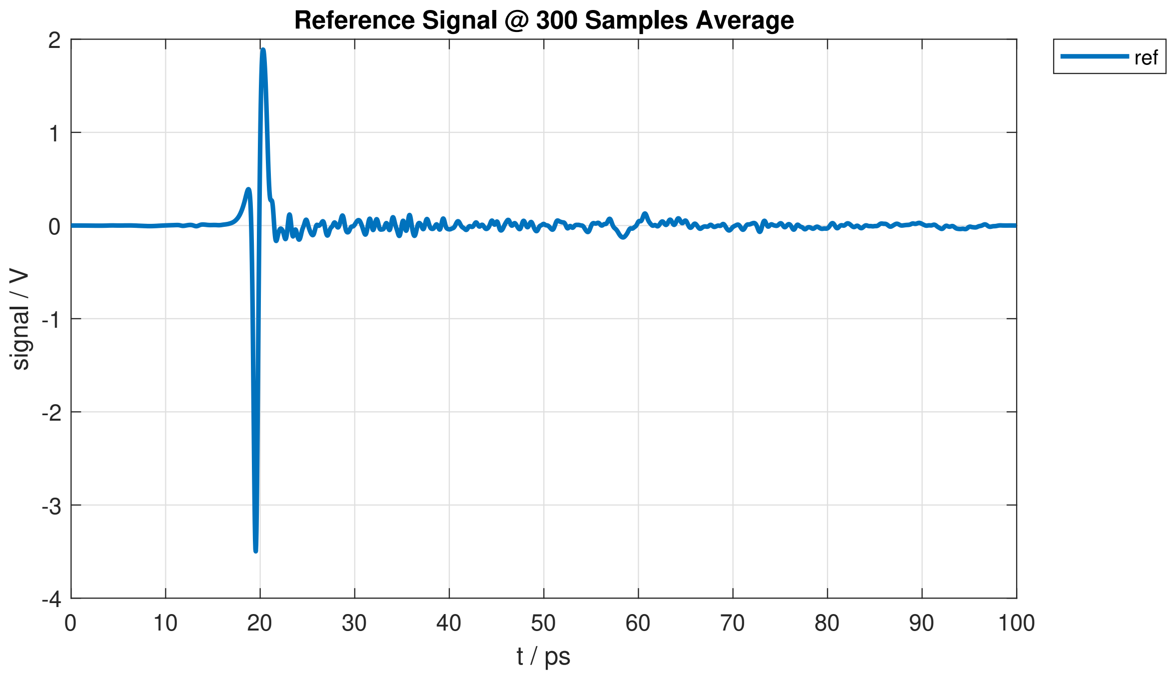

Fig. 1. Reference signal with the aligned PCAs and lenses.

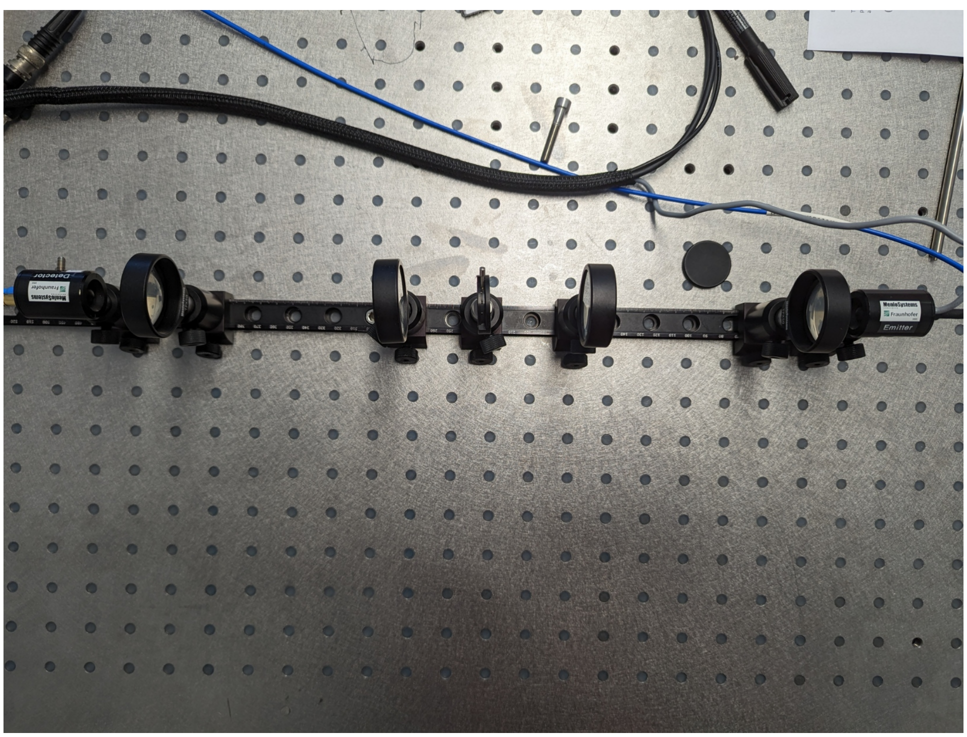

Fig. 2. PCAs and lenses setup after alignment.

II. Material Permittivity Characterization

The placement of the material introduces a delay in the system's pulse response. This delay is introduced by the slower light speed inside the material. Furthermore, the speed of light inside a material is related to the refractive index $n = \sqrt{\epsilon_r}$. Therefore, by measuring the delay and knowing the width of the sample, the relative permittivity of the material is evaluated

$$\epsilon_r = (\frac{c_0(\tau_d + \tau_0)}{d})^2, \tag{1}$$

where τ_d and τ_0 are the time it takes for the beam to go through the sample and over the air for the sample's thickness, and d is the sample's thickness.

Although, time-gating is not necessary for evaluating the material's permittivity, as only the delay in the pulse response is needed, time-gating can be applied to the reference and sample signals, in order to remove noise and scattering.

A. Sample A

The reference and sample signals of sample A (also called grey) are plotted in Fig.3. Based on the delayed pulse response, the sample has a permittivity of around $\epsilon_r = 11.29$ and is concluded to be silicon.

B. Sample B

The reference and sample signals of sample B (also called square) are plotted in Fig.4. Based on the delayed pulse response, the sample has a permittivity of around $\epsilon_r = 1.32$ and is concluded to be Gore-Tex.

C. Sample C

The reference and sample signals of sample C (also called white) are plotted in Fig.5. Based on the delayed pulse response, the sample has a permittivity of around $\epsilon_r = 2.09$ and is concluded to be teflon.

D. Conclusions

The characterized materials are silicon (sample A), Gore-Tex (sample B), and teflon (sample C) respectively. The materials and their relative permittivity are summarized in Table.III.

The code used to characterize the permittivity and material is shown in Appendix.A.

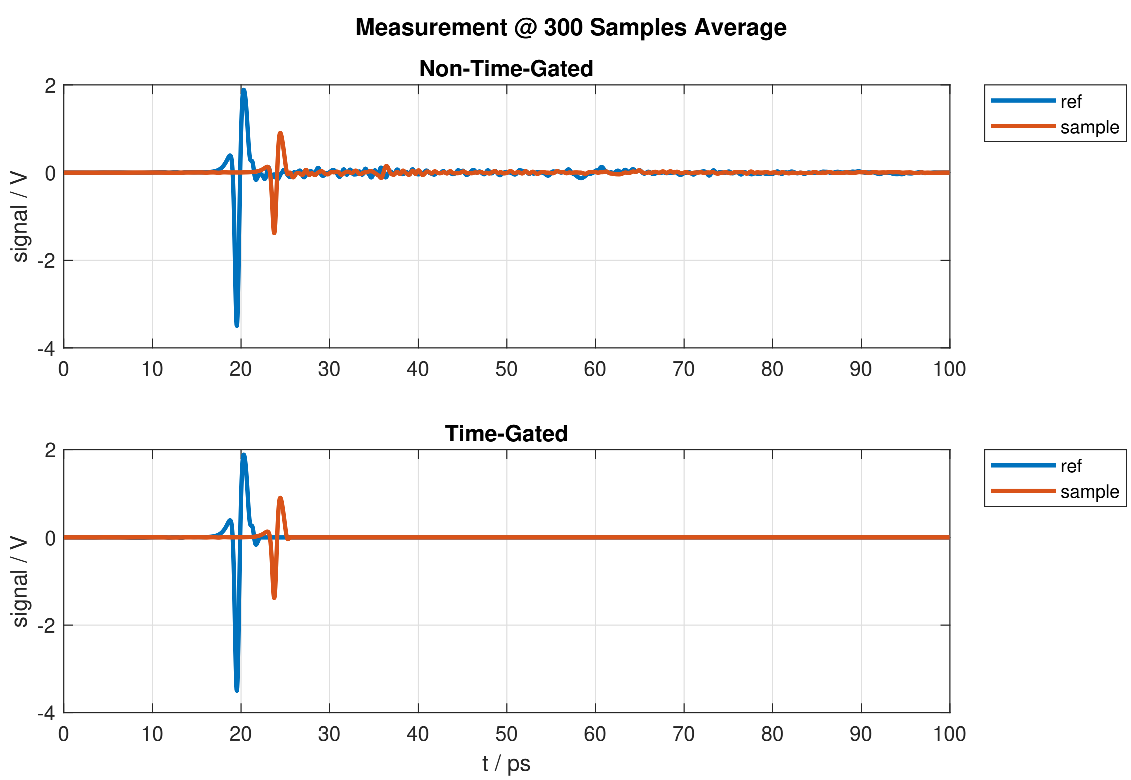

Fig. 3. Reference and sample signals for sample A (grey).

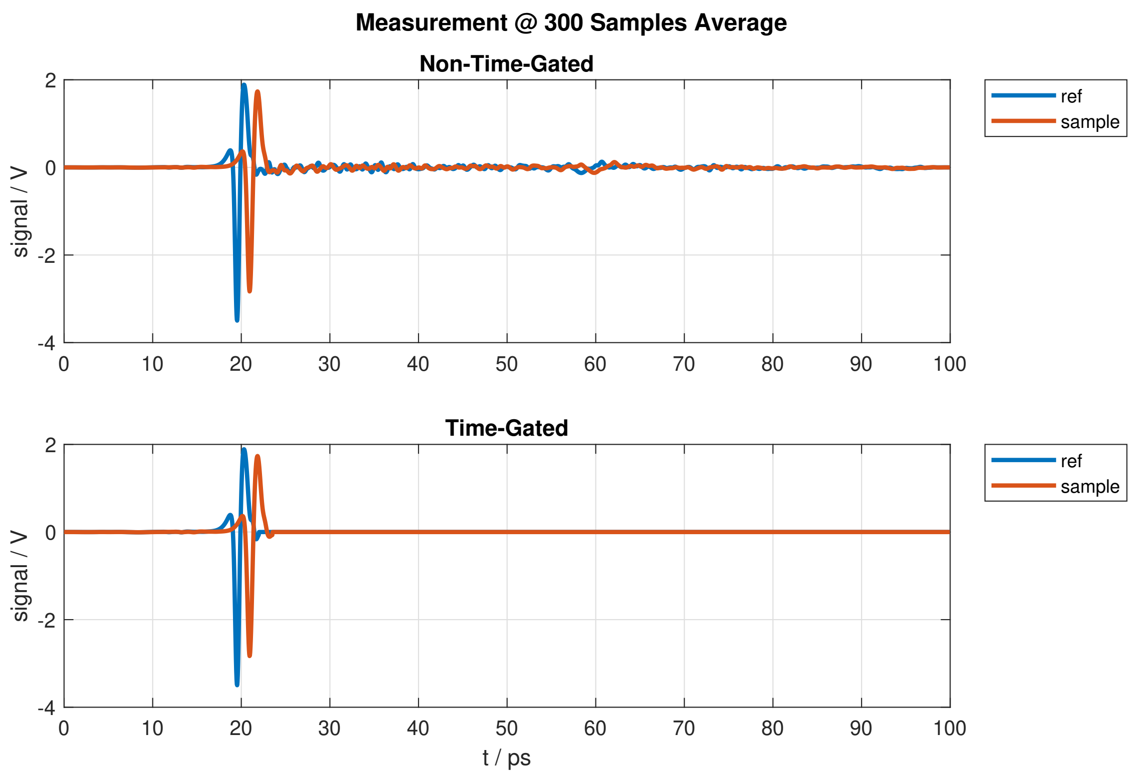

Fig. 4. Reference and sample signals for sample B (square).

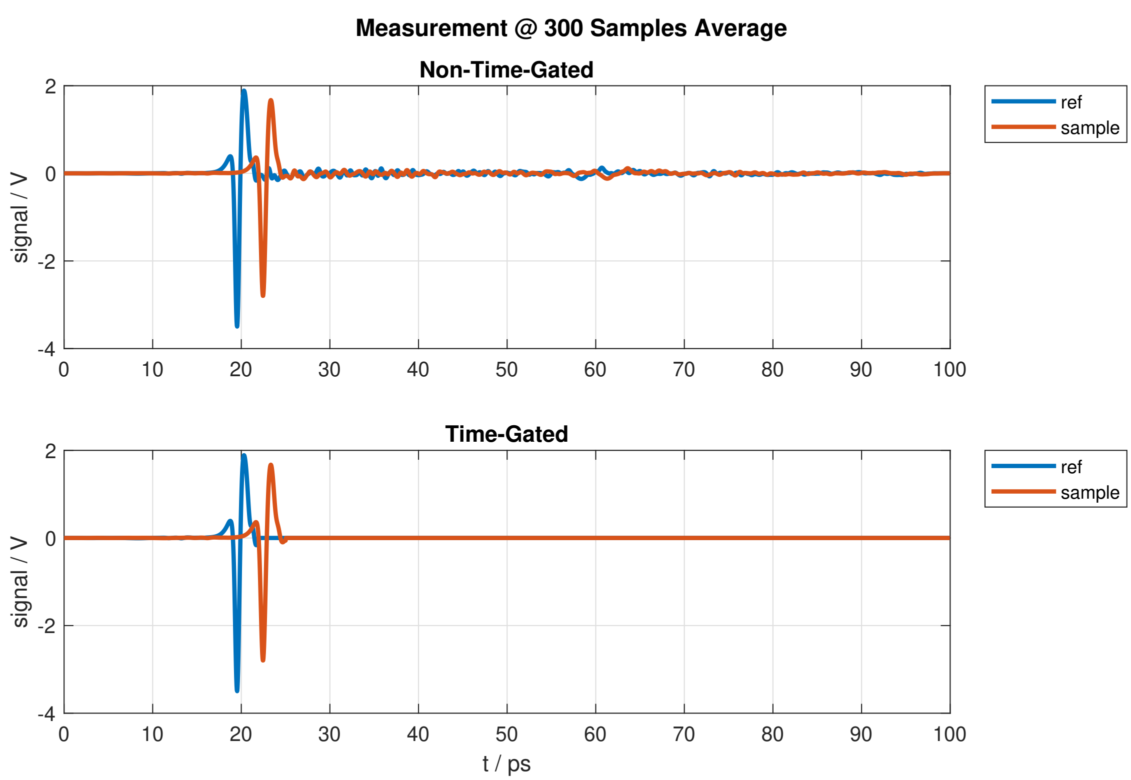

Fig. 5. Reference and sample signals for sample C (white).

TABLE III
PERMITTIVITY AND MATERIAL CHARACTERIZATION OF SAMPLES.

Samples			
	Sample A	Sample B	Sample C
ϵ_r	11.29	1.32	2.09
Material	silicon	Gore-Tex	teflon

III. LOSS TANGENT CHARACTERIZATION

The placement of the material introduces losses in the beam's propagation path. Moreover, this propagation path can be modelled using a transmission line mode consisting of a semi-infinite free space medium, followed by the sample's medium, and then followed by another semi-infinite free space medium. Therefore, using this transmission line model, the loss tangent and attenuation constant of the material are characterized.

The difference between the input and output forward propagating waves (input is defined as the wave incident on the dielectric from the first free space medium, and output as the wave transmitted from the dielectric to the second free space medium) is defined by the ratio of the sample's transmission parameter and the reference transmission parameter

$$\frac{V_{out}^{+}}{V_{in}^{+}} \approx \frac{S_{21}^{samp}(f)}{S_{21}^{ref}}, \tag{2}$$

where the transmission parameter is the frequency response of the measured pulse response, the Fourier Transform (FT) of the pulse response.

From the defined TL model, the ratio between the input and output forward propagating waves is defined by the reflection coefficients at the two interfaces, the attenuation, and the phase change terms

$$\frac{V_{in}^{+}}{V_{out}^{+}} = \frac{e^{jk_{zd}d}e^{-jk_{z0}d}}{1+\Gamma_2}\frac{1+\Gamma_1 e^{-jk_{zd}2d}}{1+\Gamma_1}, \tag{3}$$

where Γ_1 and Γ_2 are defined as the reflection coefficients at the first and second interface respectively as seen from the transmission PCA, and k_{zd} and k_{z0} are the propagation constant inside the dielectric and free space respectively. The reflection coefficient at the interfaces ones and two are related to the wave impedance inside free space and samples

$$\Gamma_1 = \frac{Z_{in}^{1} - Z_0}{Z_{in}^{1} + Z_0}, \tag{4a}$$

$$\Gamma_2 = \frac{Z_0 - Z_d}{Z_0 + Z_d}, \tag{4b}$$

where Z_{in}^{1} is the input impedance seen at interface one, and Z_0 and Z_d are the wave impedance in free space and the sample respectively. Moreover, the input impedance at interface one is the related to the free space and sample wave impedance

$$Z_{in}^{1} = Z_d \frac{Z_0 + jZ_d \tan(k_{zd}d)}{Z_d + jZ_0 \tan(k_{zd}d)}. \tag{5}$$

The wave impedance inside the dielectric has a real and imaginary part due to the losses

$$Z_d = \frac{Z_0}{\sqrt{\epsilon_r}}(1 + j\frac{\tan\delta}{2}), \tag{6}$$

where $\tan\delta$ is the loss tangent. In addition, naturally, the propagation constant inside the dielectric is related to the attenuation constant

$$k_{zd} = \beta_d - j\alpha_d = \omega\sqrt{\mu_0\epsilon_0\epsilon_r}(1 + j\frac{\tan\delta}{2}), \tag{7}$$

where ω is the angular frequency and ϵ_r is the previously evaluated relative permittivity of the material.

Arriving to analytical solution for the loss tangent is complex, therefore, it is evaluated by generating a set of values, calculating the ratio between the input and output forward propagating waves as defined in Eq.3. The ratios are complex, due to containing phase term, consequently, the loss tangent is evaluated by comparing each absolute value calculated according to the TL model and the measurement (this is performed by selecting the value that is closer to zero when taking the difference between the two). The code used to characterize the loss tangent and attenuation constant is shown in Appendix.B.

A. Silicon (Sample A, grey)

The pulse response's spectrum of the silicon sample is plotted in Fig.6. Its evaluated loss tangent is plotted in Fig.7. Moreover, the attenuation constant of the same sample is plotted in Fig.8.

B. Gore-Tex (Sample B, square)

The pulse response's spectrum of the Gore-Tex sample is plotted in Fig.9. Its evaluated loss tangent is plotted in Fig.10. Moreover, the attenuation constant of the same sample is plotted in Fig.11.

C. Teflon (Sample C, white)

The pulse response's spectrum of the teflon sample is plotted in Fig.12. Its evaluated loss tangent is plotted in Fig.13. Moreover, the attenuation constant of the same sample is plotted in Fig.14.

D. Conclusions

The material with highers losses is silicon, followed by teflon, and lastly Gore-Tex. Evaluation of the loss tangent and attenuation constant with time-gated pulse response are plotted in Appendix.C.

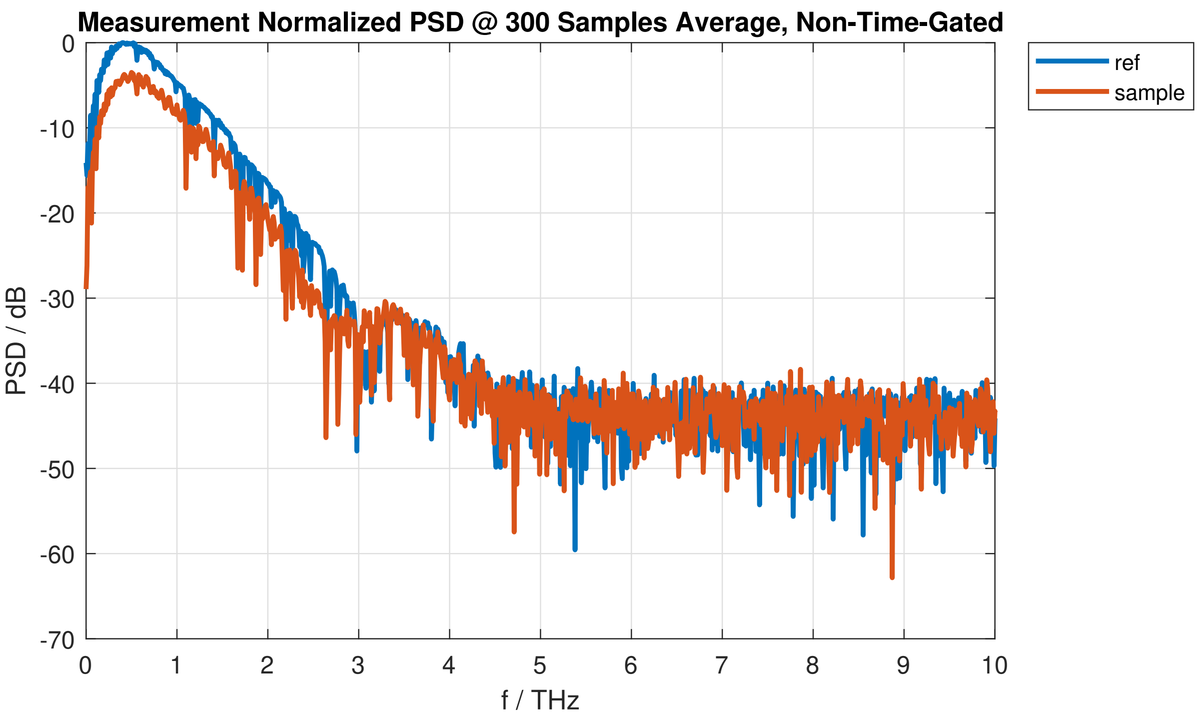

Fig. 6. Power spectrum density of pulse response with silicon (sample A, grey) and non-time-gated time domain signal.

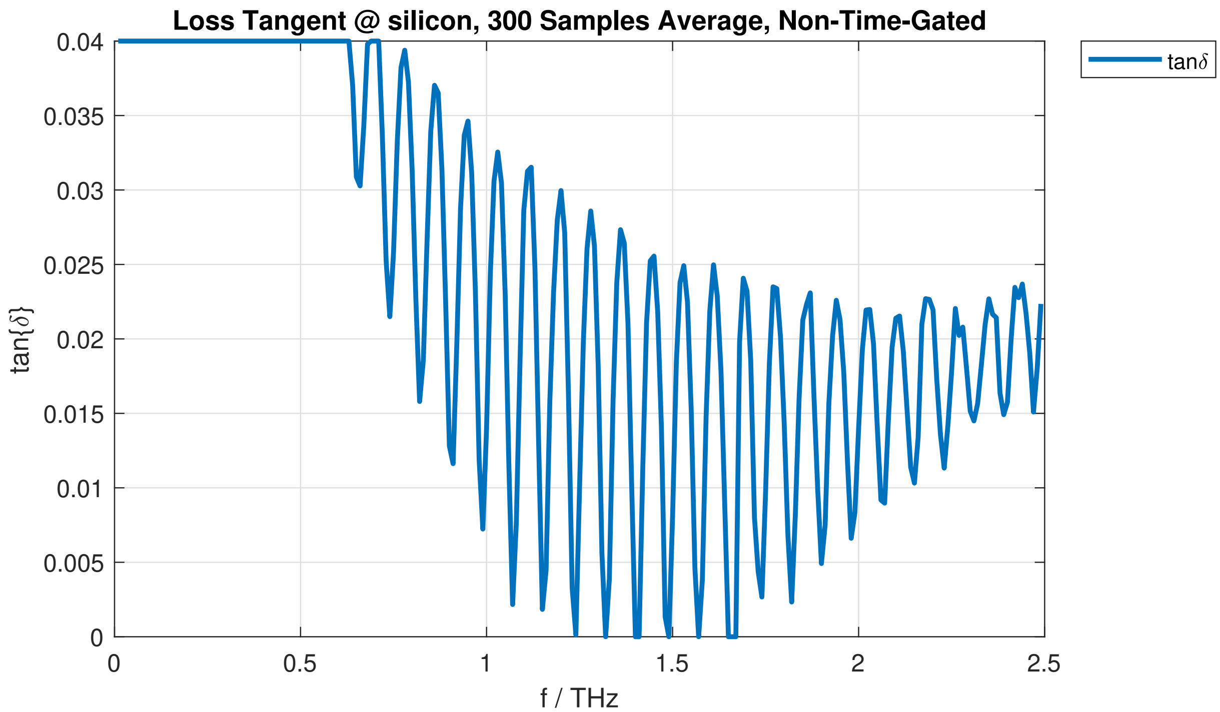

Fig. 7. Evaluated loss tangent of silicon (sample A, grey) with non-time-gated time domain signal.

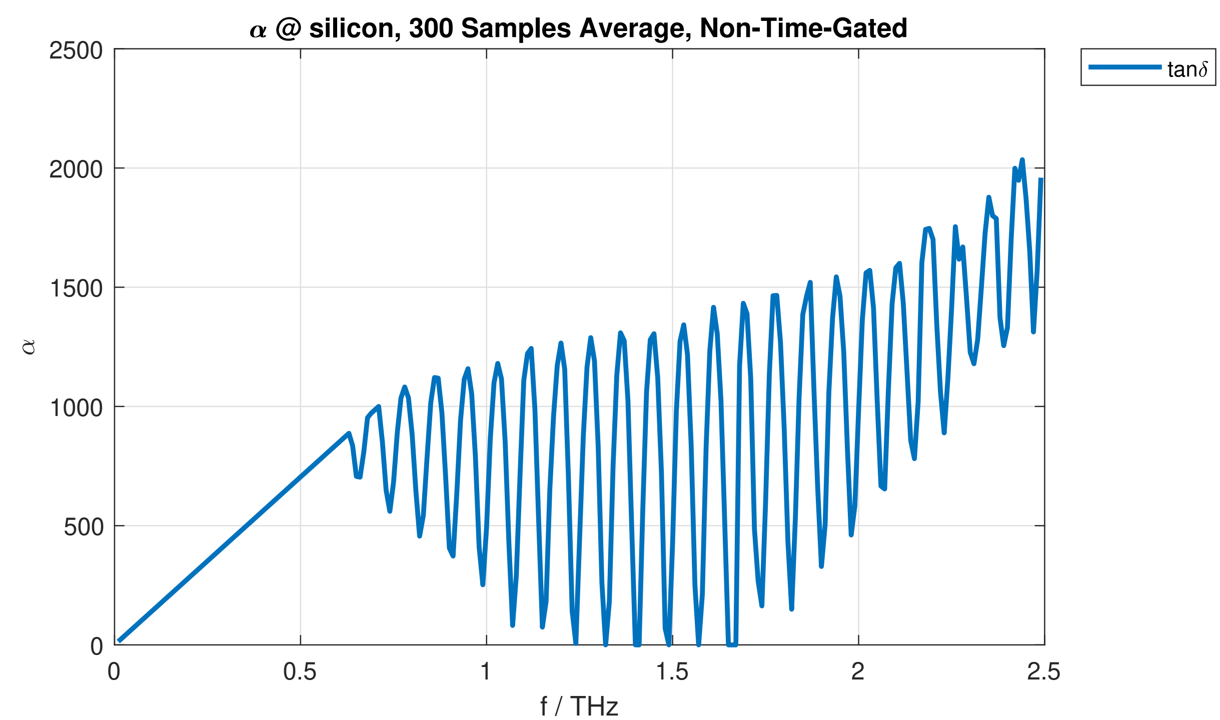

Fig. 8. Evaluated attenuation constant of silicon (sample A, grey) with non-time-gated time domain signal.

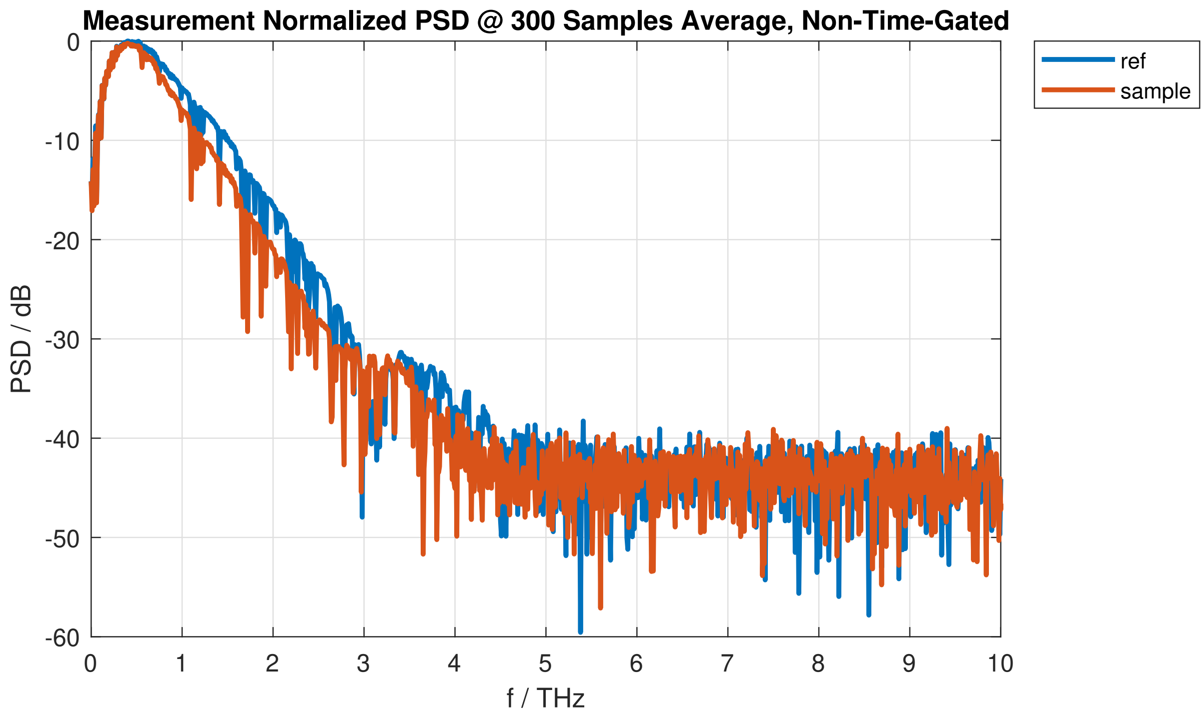

Fig. 9. Power spectrum density of pulse response with Gore-Tex (sample B, square) and non-time-gated time domain signal.

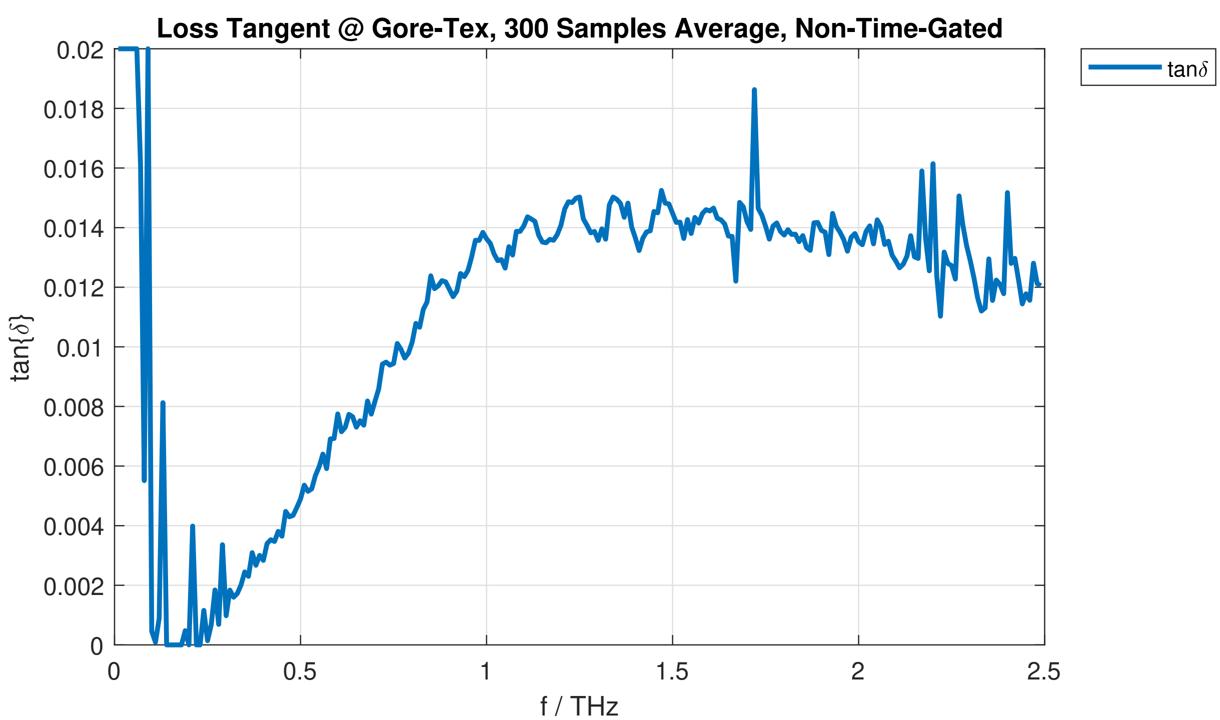

Fig. 10. Evaluated loss tangent of Gore-Tex (sample B, square) with non-time-gated time domain signal.

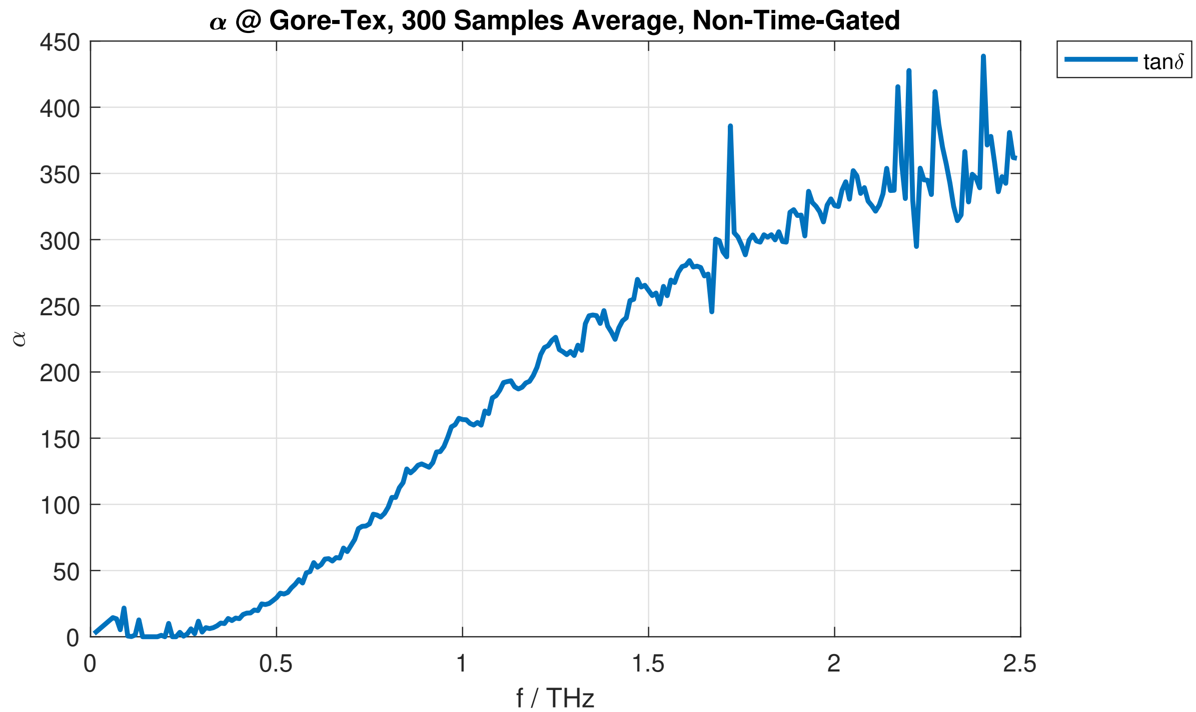

Fig. 11. Evaluated attenuation constant of Gore-Tex (sample B, square) with non-time-gated time domain signal.

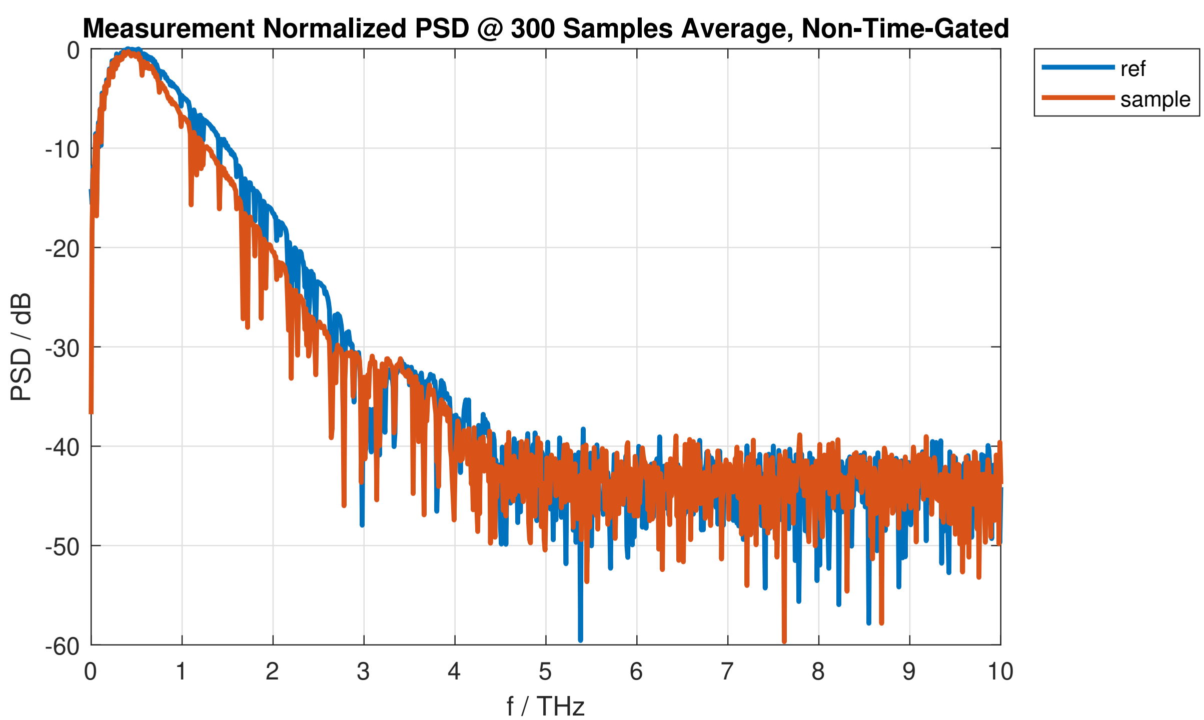

Fig. 12. Power spectrum density of pulse response with teflon (sample C, white) and non-time-gated time domain signal.

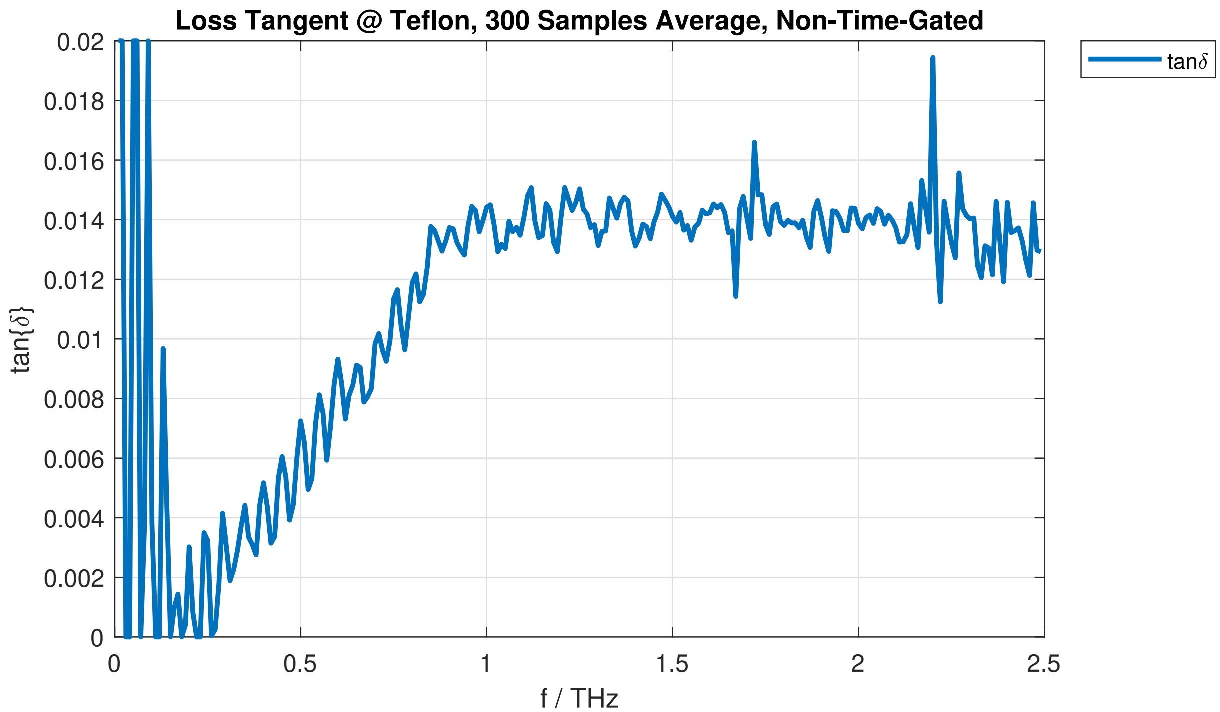

Fig. 13. Evaluated loss tangent of teflon (sample C, white) with non-time-gated time domain signal.

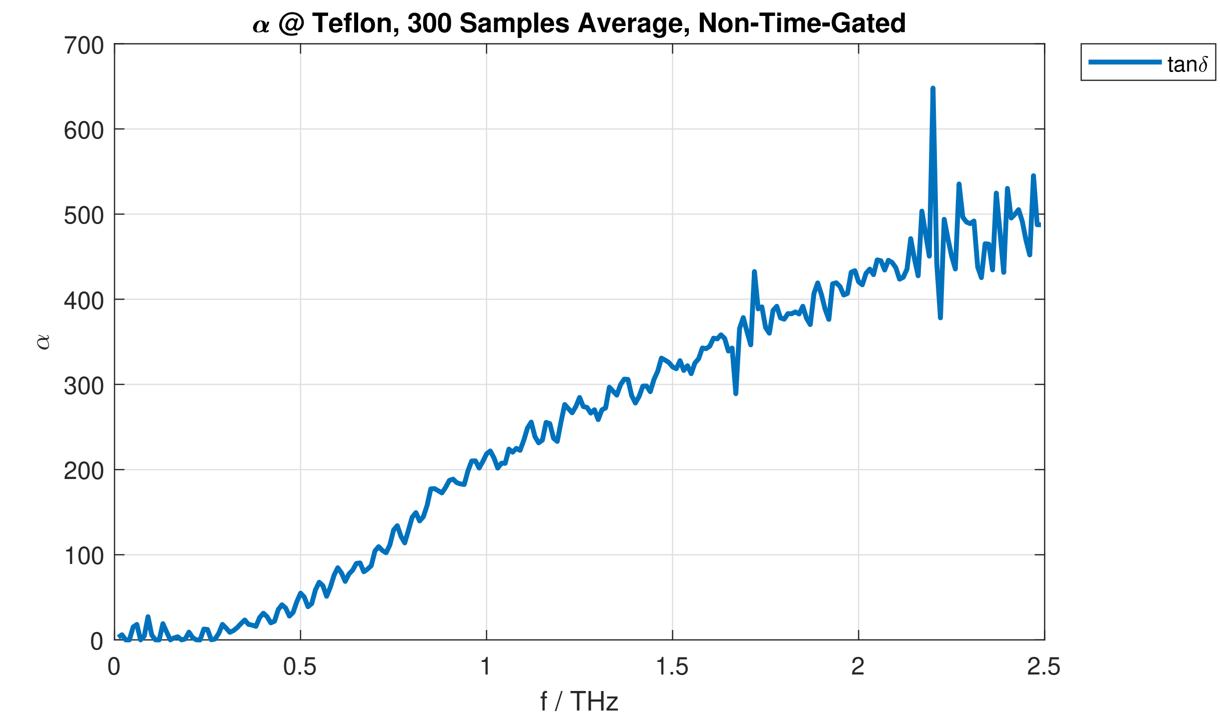

Fig. 14. Evaluated attenuation constant of teflon (sample C, white) with non-time-gated time domain signal.

APPENDIX A
PERMITTIVITY CODE SNIPPET

The **MatLab** code used to perform permittivity and material characterization is shown below. The functions and scripts used for the post-processing are at time-domain-lab.

```
c = physconst('LightSpeed');

[ref_pks, ref_idx_pks] = findpeaks(reference.s);
[~, ref_idx_max_pk] = max(ref_pks);
ref_loc_pk = ref_idx_pks(ref_idx_max_pk);

[sample_pks, sample_idx_pks] = findpeaks(sample.s);
[~, sample_idx_max_pk] = max(sample_pks);
sample_loc_pk = sample_idx_pks(sample_idx_max_pk);

time_diff = sample.t(sample_loc_pk) - reference.t(ref_loc_pk);
time_air = sample_width / c;
sample_permittivity = (c * (time_diff + time_air) / sample_width) ^ 2;

[~, idx] = min(abs(permittivity_list.permittivity - sample_permittivity));
material = permittivity_list.material(idx);
```

APPENDIX B
LOSS TANGENT AND ATTENUATION CONSTANT CODE SNIPPET

The **MatLab** code used to perform permittivity and material characterization is shown below. The functions and scripts used for the post-processing are at time-domain-lab.

```
c = physconst('LightSpeed');
e0 = 8.8541878128 * 1e-12;
u0 = 1.25663706212 * 1e-6;
Z0 = 376.730313668;

er = sample.er;

freq = reference.f(reference.f <= freq_limit);
num_freq_pts = length(freq);

loss_tangent = linspace(bounds(1), bounds(2), tand_pts);

ref_fft = reference.fft(reference.f <= freq_limit);
sample_fft = sample.fft(reference.f <= freq_limit);

tand = NaN(1, num_freq_pts);
alpha = NaN(1, num_freq_pts);

for freq_idx = 2 : 1 : num_freq_pts
    w = 2 * pi * freq(freq_idx);
    lambda = c / freq(freq_idx);
    kz0 = 2 * pi / lambda;

    % Wave parameters inside dielectric
    Zd = (Z0 / sqrt(er)) * (1 + 1j * loss_tangent / 2);
    alpha_d = w * sqrt(e0 * u0 * er) * loss_tangent / 2;
    beta_d = w * sqrt(e0 * u0 * er);
    kzd = beta_d - 1j * alpha_d;

    % Interface 2, dielectric-air parameters
    gamma_B = (Z0 - Zd) ./ (Z0 + Zd);
```

```
    Vs_Vout = exp(1j * kzd * d) .* exp(- 1j * kz0 * d) ./ (1 + gamma_B);

    % Interface 1, air-dielectric parameters
    Zin_A = Zd .* (Z0 + 1j * Zd .* tan(kzd * d)) ./ (Zd + 1j * Z0 .* tan(kzd * d));
    gamma_A = (Zin_A - Z0) ./ (Zin_A + Z0);
    Vin_Vs = (1 + gamma_B .* exp(-1j * kzd * 2 * d)) ./ (1 + gamma_A);

    Vin_Vout = abs(Vin_Vs .* Vs_Vout);
    Vout_Vin_meas = abs(ref_fft(freq_idx) / sample_fft(freq_idx));

    [~, tand_idx] = min(abs(Vin_Vout - Vout_Vin_meas));
    tand(freq_idx) = loss_tangent(tand_idx);
    alpha(freq_idx) = alpha_d(tand_idx);
end
```

Appendix C
Loss Tangent And Attenuation Constant Evaluation Using Time-Gated Signals

The figures with the evaluation of the loss tangents and attenuation constants using time-gated pulse response signals are the following.

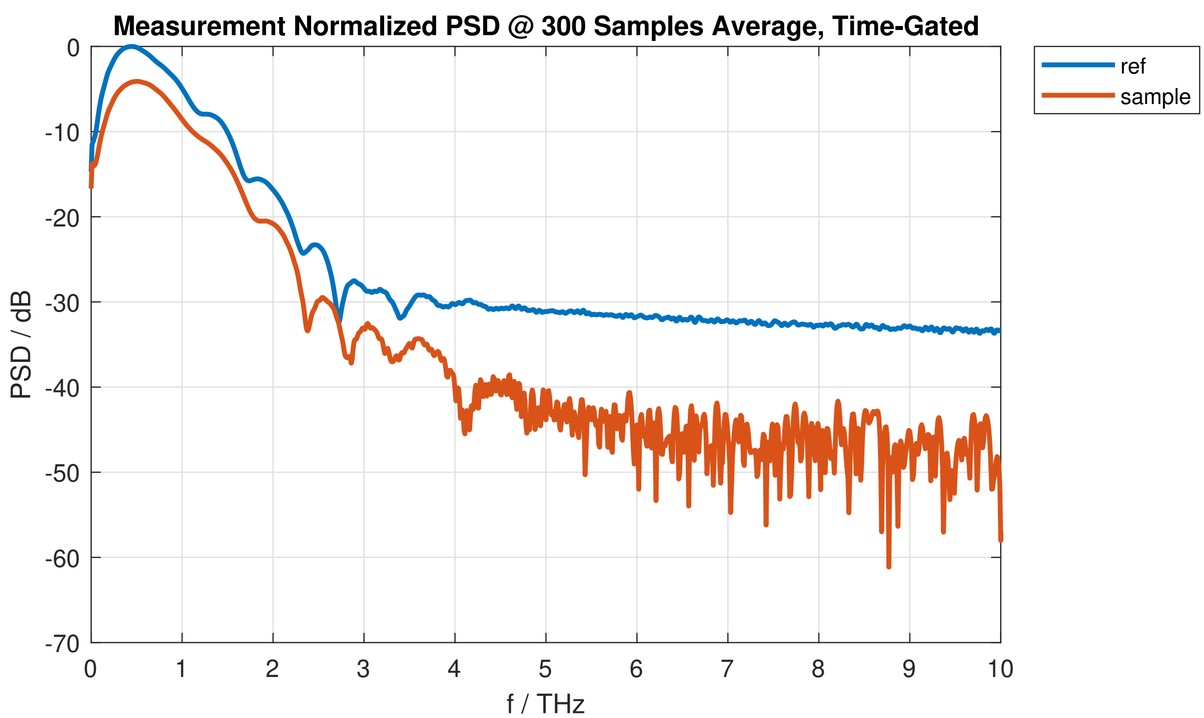

Fig. 15. Power spectrum density of pulse response with silicon (sample A, grey) and time-gated time domain signal.

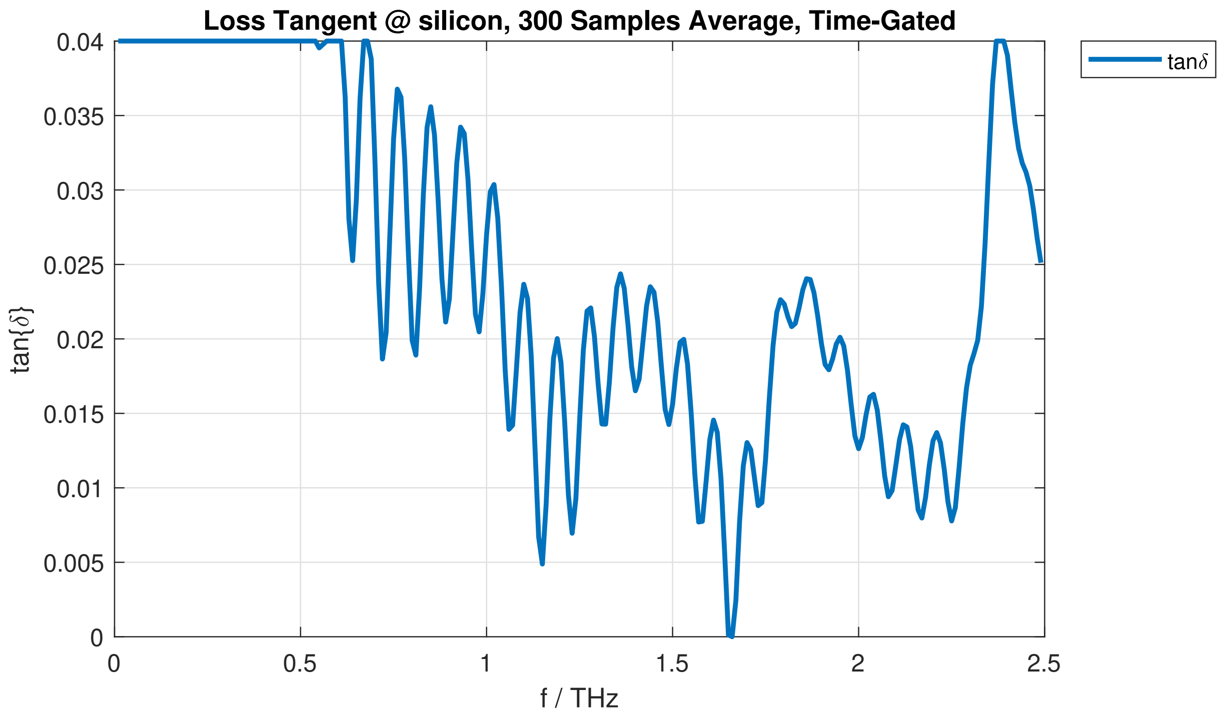

Fig. 16. Evaluated loss tangent of silicon (sample A, grey) with time-gated time domain signal.

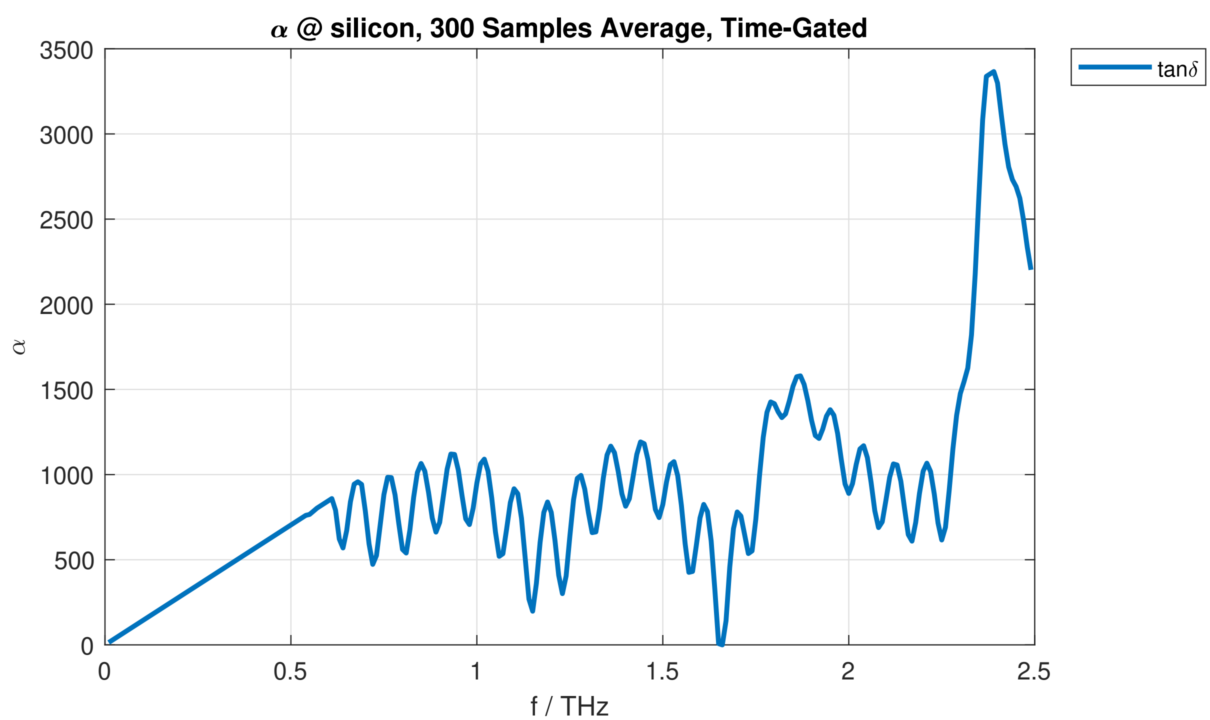

Fig. 17. Evaluated attenuation constant of silicon (sample A, grey) with time-gated time domain signal.

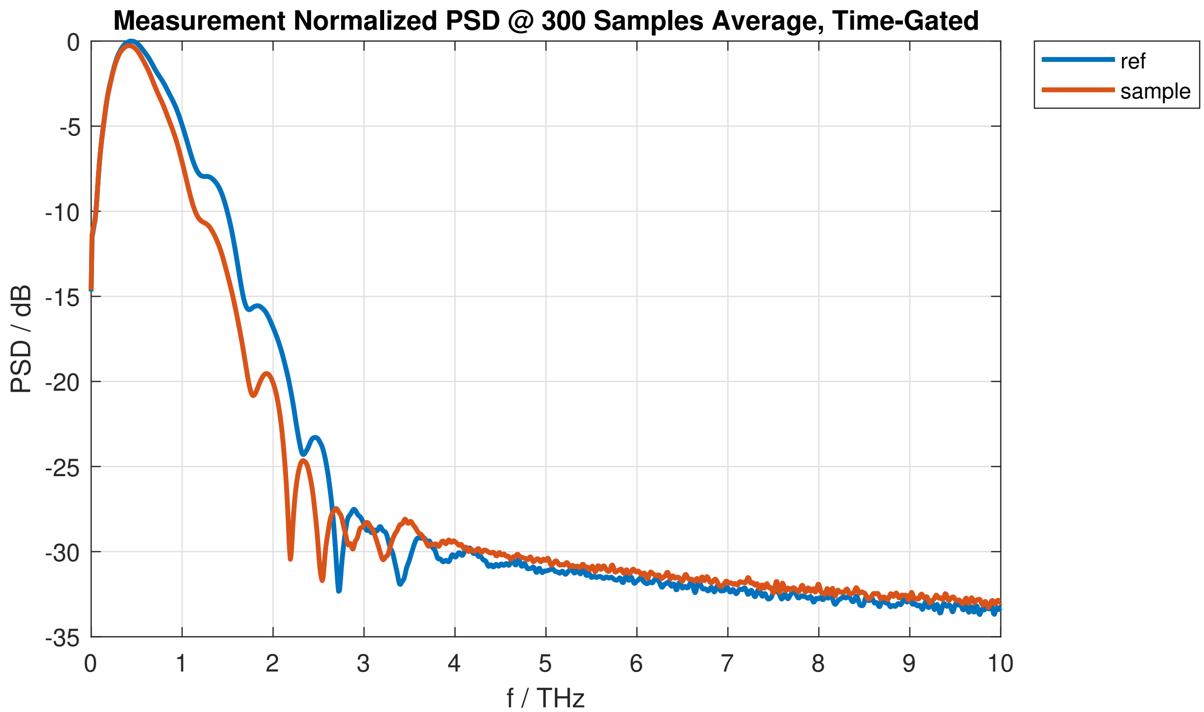

Fig. 18. Power spectrum density of pulse response with Gore-Tex (sample B, square) and time-gated time domain signal.

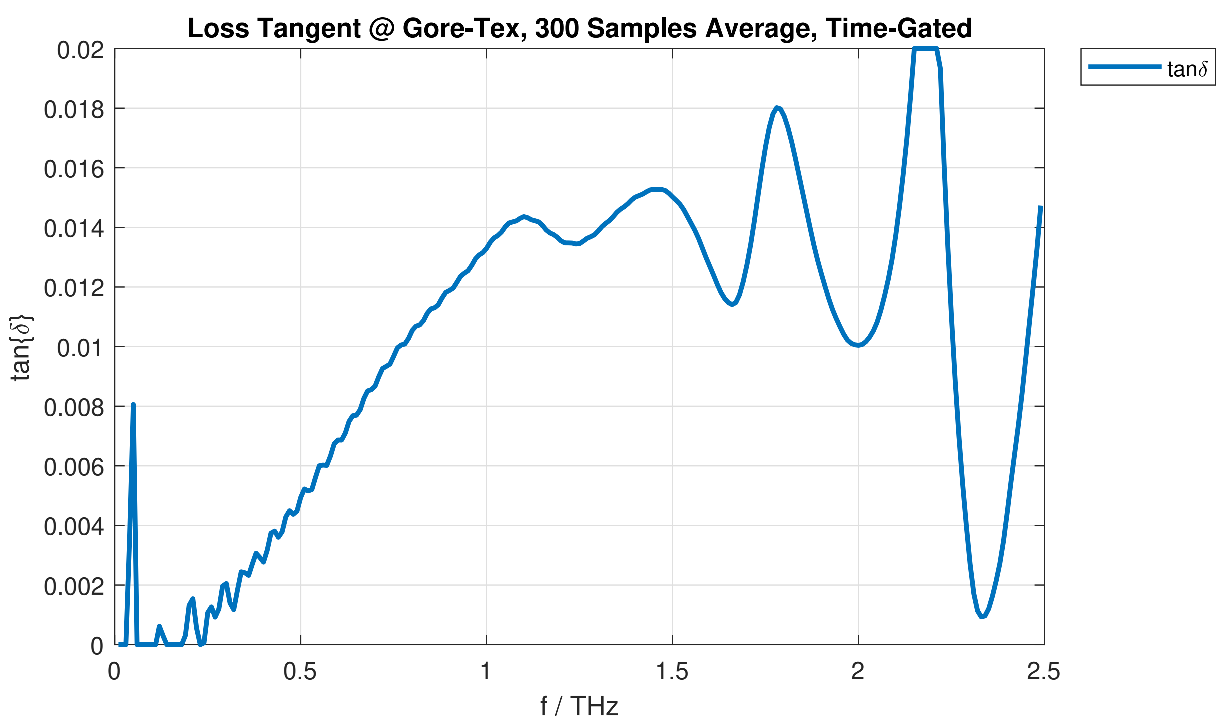

Fig. 19. Evaluated loss tangent of Gore-Tex (sample B, square) with time-gated time domain signal.

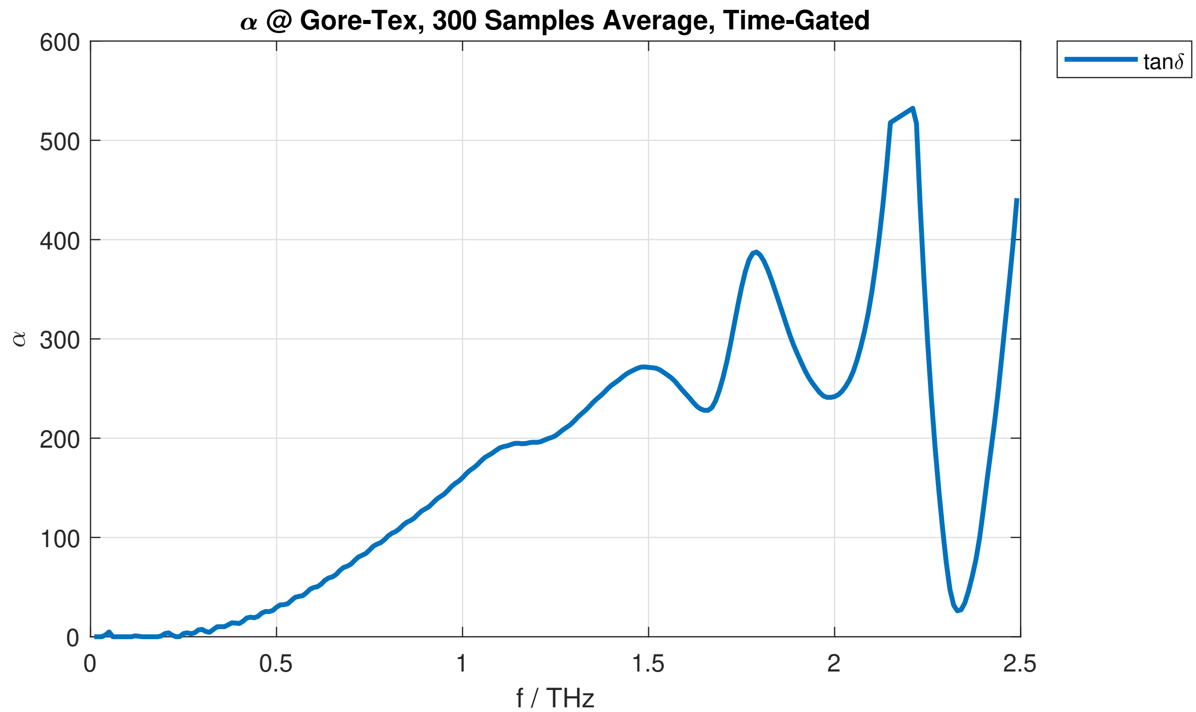

Fig. 20. Evaluated attenuation constant of Gore-Tex (sample B, square) with time-gated time domain signal.

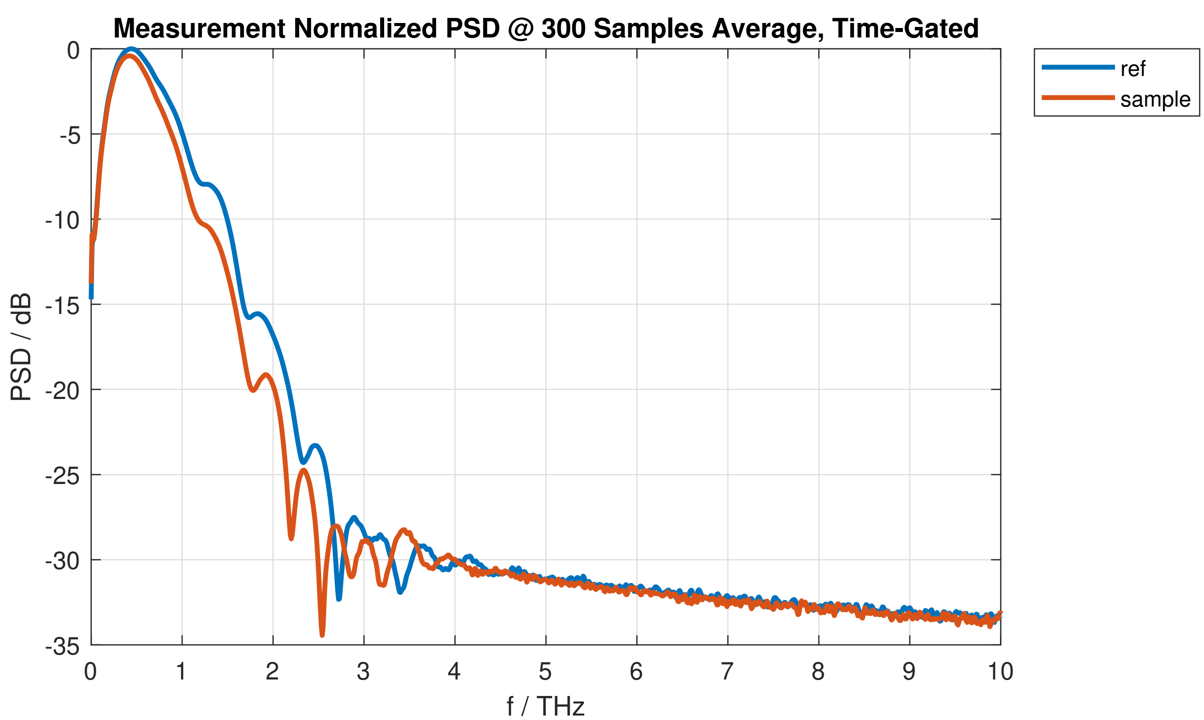

Fig. 21. Power spectrum density of pulse response with teflon (sample C, white) and time-gated time domain signal.

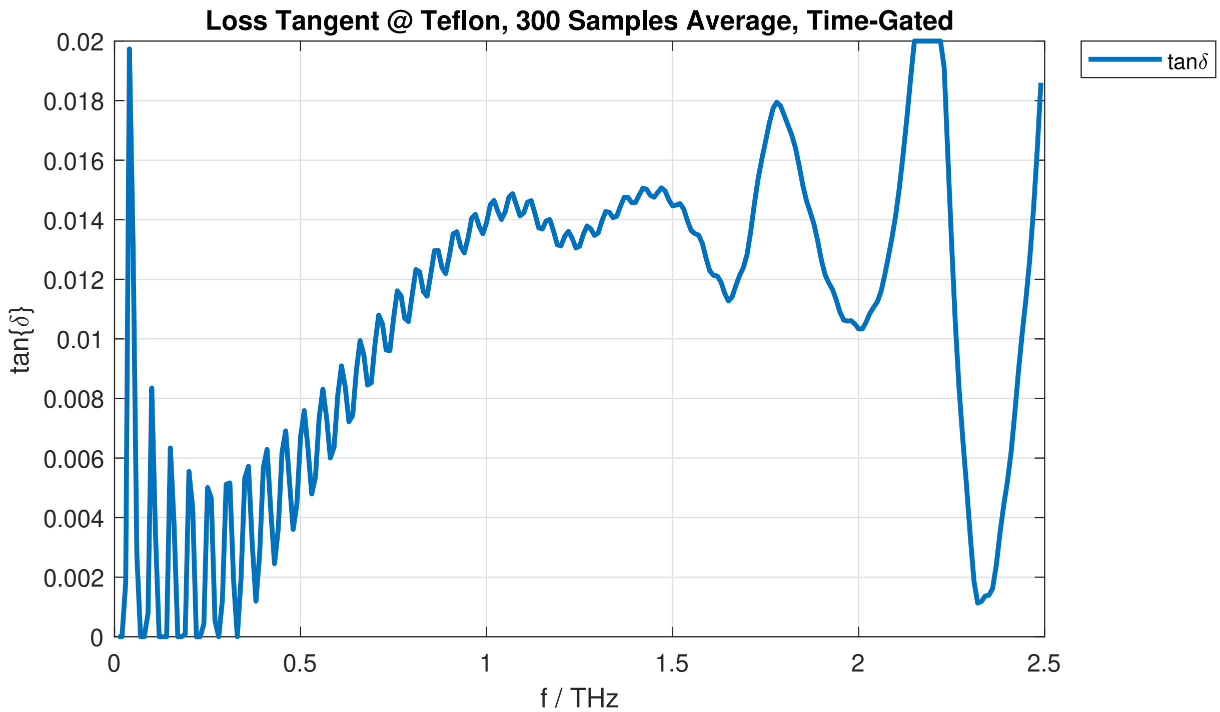

Fig. 22. Evaluated loss tangent of teflon (sample C, white) with time-gated time domain signal.

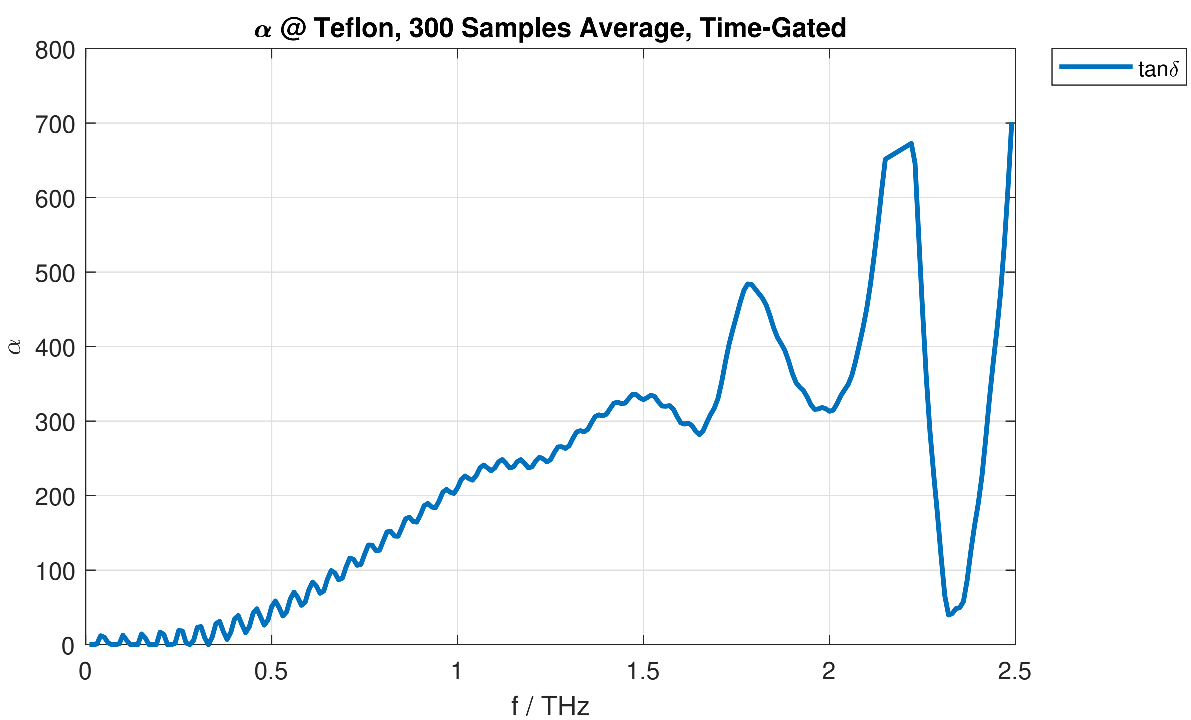

Fig. 23. Evaluated attenuation constant of teflon (sample C, white) with time-gated time domain signal.